Impact of compressibility in vertically integrated models for CO_2 storage

Master Thesis in
Applied and Computational Mathematics

by

Silje Rognsvåg Reistad

June, 2012

Department of Mathematics
University of Bergen
Norway

Abstract

Recent work have shown that simplified models obtained by vertical integration give reasonable approximations for CO_2 migration. Most of the work previously done on this topic assumes that CO_2 is an incompressible fluid, or they work with a quasi compressibility, where they consider horizontal compressibility but not vertical. However, CO_2 is highly compressible and large variations in CO_2 density can be expected due to pressure increases near the injection well. In addition, long term CO_2 migration to shallower depths can result in significantly lower density as dictated by geothermal gradients and regional pressure conditions. In this study, we outline the mathematical and numerical approach to solve the coupled vertically integrated models with density variation. Mathematical models for CO_2 storage are considered in which the equations for mass conservation and Darcy's law are vertically integrated and coupled with an equation of state for CO_2 density. Based on these, a pressure equation is derived. This pressure equation is then discretised with the use of an implicit control volume method and a partially implicit Lax-Friedrichs' method. A solution approach based on an IMPES approach is suggested.

We have unfortunately not been able to solve this problem, as there has been some difficulties with the boundary values in the code, but we suggest a plan for further work for a working code.

Acknowledgements

First of all, I would like to thank my supervisors, Jan, Sarah and Helge, for their help in this work, and especially for giving me the opportunity to travel and experience so much during these two years of working on my master thesis. In particular for the trip to Minneapolis is June 2011, and to the Winter School at Geilo January 2011. Also thanks to all my fellow students, and in particular my room-mates and lunch-mates.

Most of all, I would like to say thank you to my family. My parents for always showing interest in my work, even though they have no idea what I am talking about, and in particular my amazing husband Jone. Without you, I would never have gotten this far!

Silje Rognsvåg Reistad,
Bergen, June 2012

Contents

Chapter 1

Background

1.1 The Carbon Problem

The carbon problem refers to the increase of the green house gas CO_2 in the atmosphere over the last 200 years. The concentration of CO_2 has a natural variation from year to year, but lately we have seen a dramatic increase over a short period of time. Figure 1.1 shows measurements done on Mauna Loa, Hawaii, and we can clearly see how the concentration of CO_2 has increased over the last 50 years. To put this in a more historical context, we look at data from samples of polar ice. Figure 1.2 shows the result of these measurements and indicate the CO_2 concentration in the atmosphere over the last 100 years. As we can see from the figure, the concentration of CO_2 started increasing from historical values around year 1800, which was the time of the industrial revolution. Today, the CO_2 concentration is around 100 parts per million (ppm) above what it was before 1800.

Looking at these two figures, there is no doubt in anyone's mind that the atmospheric concentration of CO_2 has increased. What researchers disagree on, is whether this increase has a negative effect on the world's climate. Whether it does or not, we do not know for sure, but are we willing to continue this global experiment to find out? Data from the International Energy Agency (IEA) shows that around 40 % of the carbon dioxide emission comes from production of electricity [*Celia and Nordbotten*, 2012]. Therefore, it seams reasonable that an effort to slow down the rapid increase of CO_2 concentration in the atmosphere should include decarbonising of this industry. One such method could be Carbon Capture and Storage.

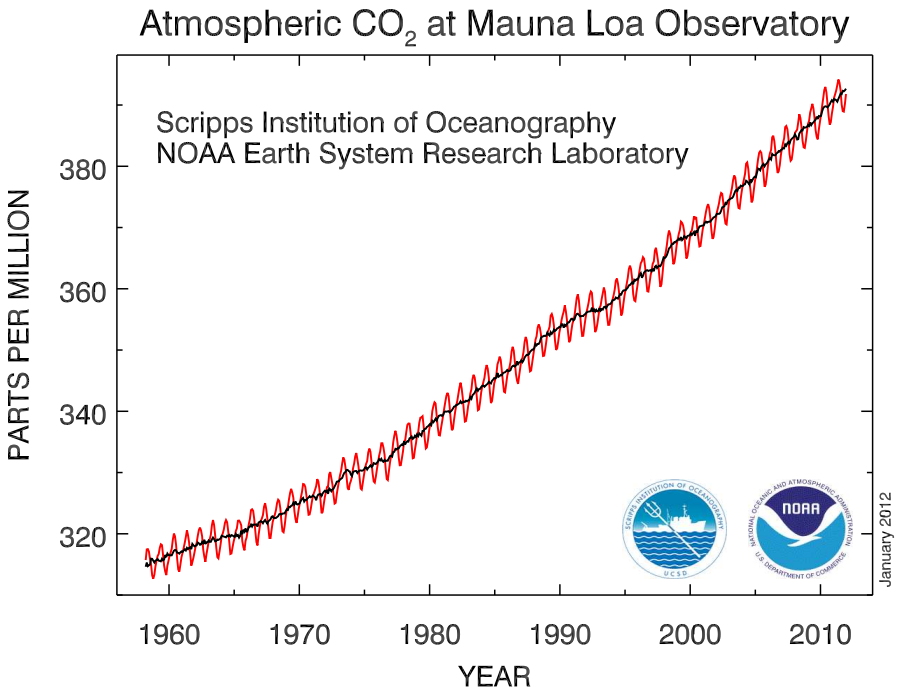

Figure 1.1: Atmospheric CO_2 concentration measured at Mauna Loa, Hawaii [*Tans and Keeling*, 2012]

1.2 Carbon Capture and Storage

Carbon Capture and Storage (CCS) involves capturing the CO_2 from burning of fossil fuels, and then store it somewhere else than in the atmosphere. It is the storage part of this process that will be investigated in this thesis. The most likely place to store the CO_2 is in deep geological formations. These formations need to be both permeable and large enough to contain large amounts of CO_2, and they also need to be overlain by a layer of lower permeability, a caprock, to keep the CO_2 in place. The CO_2 is injected through wells at a supercritical state, which means that the injected CO_2 will be significantly denser than in its gas form. CO_2 reaches a critical state when the pressure exceeds 7.4MPa, and the temperature reaches above 31.1°C as shown in Figure 1.3. For typical geothermal gradients this means that we need to inject the CO_2 in formations more than 800 m deep *Celia and Nordbotten* [2012]. Figure 1.4 shows a cartoon of such a storage process. Our aquifer is a layer, often not horizontal, but tilted, and lies between two

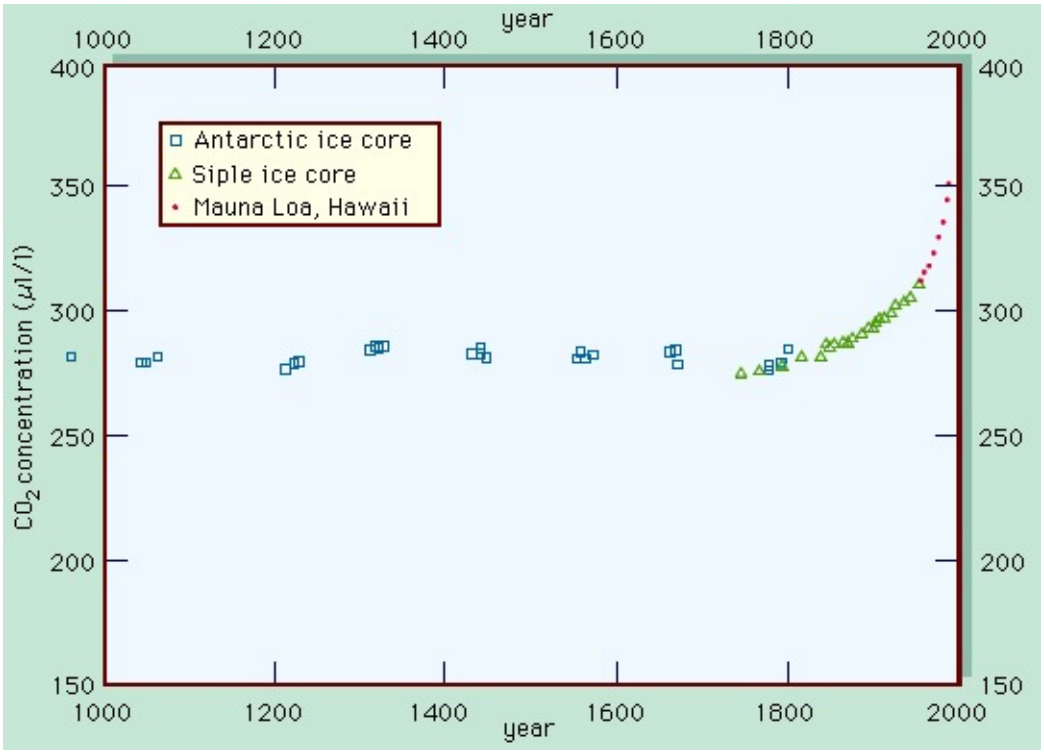

Figure 1.2: Atmospheric CO_2 concentration from ice cores coupled with measurements at Mauna Loa [*Britannica*, 2012]

impermeable (or at least low permeable) layers. The injected CO_2 will be significantly more buoyant than the brine it displaces. Therefore, the CO_2 will move away from the well, and up to the top of the aquifer. On its way, it will leave a trail of residually trapped CO_2. A typical scenario is shown in Figure 1.5.

Some CO_2 injection operations already exist. One of them is the Utsira formation, where CO_2 produced from the Sleipner gas field is injected. This project has been up and running since 1996 and has a yearly injection rate of about one million tons [*Torp and Gale*, 2002]. This is a relatively small amount compared to what is desired for future operations.

Many people have looked at these problems, among them an analytical solution by *Nordbotten et al.* [2005]. The mathematical model which describe the system is complex, and simplifications need to be made in order to solve it. Most people have decided to assume that the fluids involved in the system, CO_2 and brine, are incompressible. This is of course not the case, and in this thesis, we will look at what happens when we include compressibility in these models.

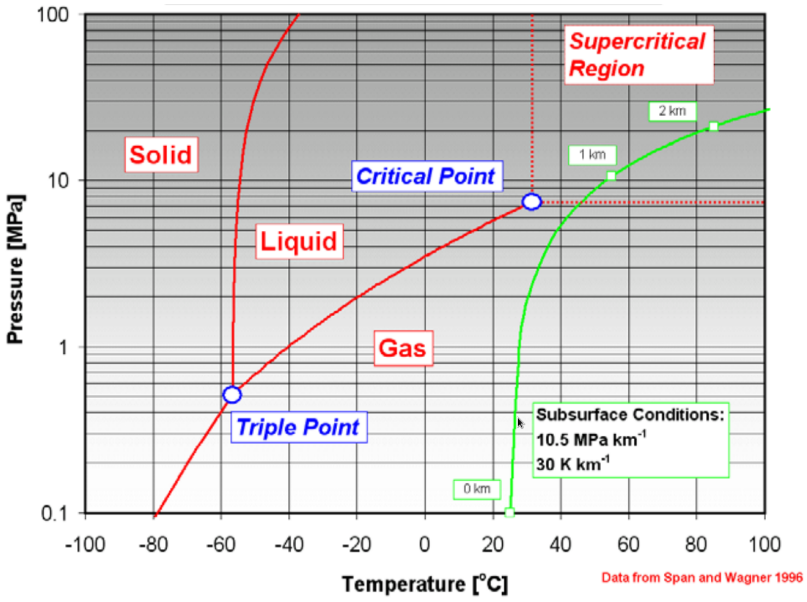

Figure 1.3: Phase diagram of CO_2 showing the temperature and the pressure in which the CO_2 is supercritical (dotted red line). The figure also shows typical subsurface conditions, where the CO_2 would be supercritical at depths below 800 m (green line). Figure from *Celia and Nordbotten* [2012]

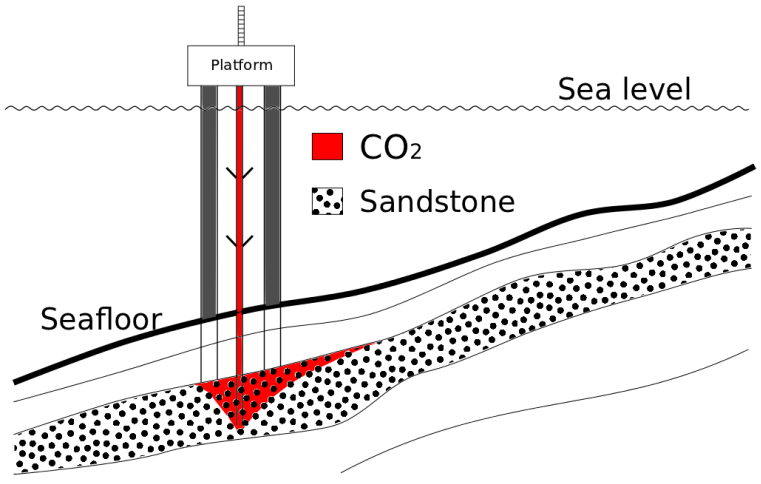

Figure 1.4: Cartoon of the CO_2 storage process, where the CO_2 is injected through a well into a high permeable aquifer deep under the surface.

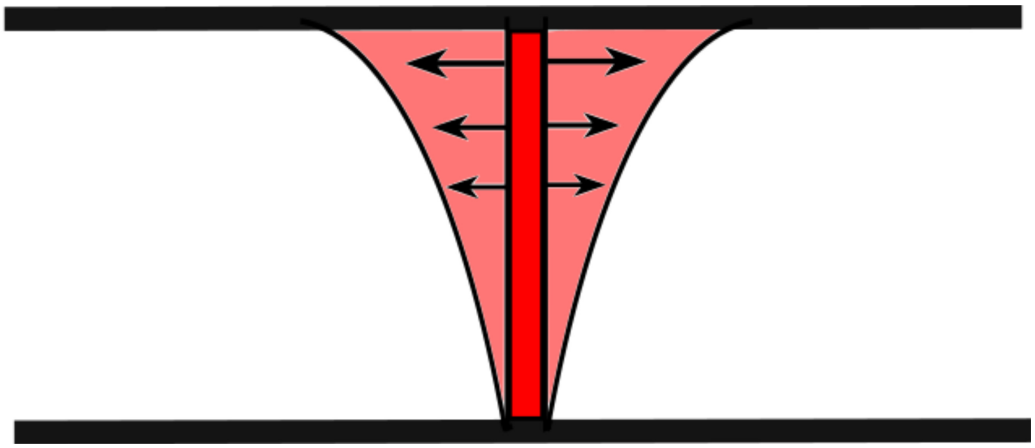

Figure 1.5: A typical scenario in CO_2 storage. The CO_2 is injected through a well in the middle of the aquifer, and will migrate upwards and outwards due to gravity and diffusion.

1.2.1 Storage processes

Figure 1.6 illustrates the different trapping mechanisms of CO_2. This will not be an important part of this thesis, but have been included to illustrate an important point. In the beginning of the storage process, most of the CO_2 is "free", meaning that it is a separate phase, and mobile to migrate outwards in the aquifer. In this early phase, the structure of the aquifer keeps the CO_2 trapped, under its overlaying caprock. It is in this period that the plume migration is most important to look at. After a while, more and more CO_2 will become trapped, either as residual CO_2 saturation as the brine imbibes to displace the CO_2, or possible dissolved in the water or trapped minerally in the aquifer.

1.3 Challenges

There are several challenges connected with large scale CCS, besides the ones involving economics and politics. One of these issues is the huge variation in the scales involved. In time scales, we need to know what will happen to the CO_2 a second after start of injection, but also where it will be thousands of years after. We also have different processes happening on completely different spatial scale, all which needs to be considered in some way.

Another thing to keep in mind, is that we need to be aware of which problem we would like to solve. For CO_2 storage sites in in the North Sea, we are worried about CO_2 leaking out and polluting the ocean, possible being

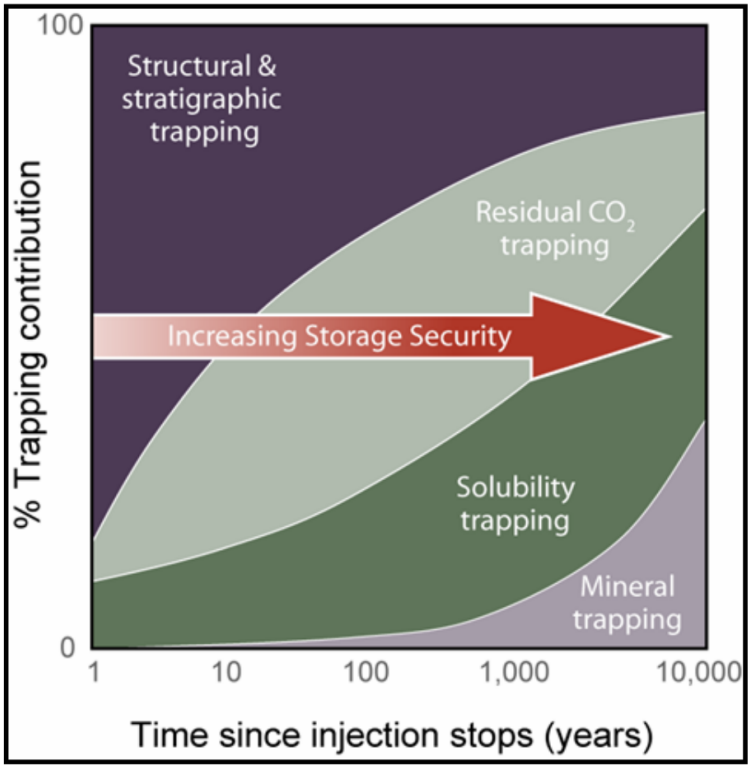

Figure 1.6: Different storage processes happening on different time scales.

a danger to animals and plants in the ocean. Brine leakage into already salty water, is less important. We are therefore interested in the migration of the CO_2 plume. However, in other possible storage sites like the Alberta basin in Canada, we are worried about brine leaking out into drinking water sources, and we are more worried about the pressure perturbations in the system. To say something about these issues, we need to make mathematical models solving the problem.

Luckily, after producing oil for decades, we already know a lot about these systems. There has been done plenty of work on this problem before, but most of these do not consider the effect of CO_2 compressibility in the system, or they use a quasi compressibility where horizontal compressibility is considered, but not vertical.

In the next chapter, we will go through some of the theory for systems of two fluids, in our case CO_2 and salty water, brine, in a porous media. This theory will form the basis of the mathematical model derived later in this thesis.

Chapter 2

Theory

We are interested in a system of two fluids, CO_2 and salty water, brine, flowing inside a sandstone, or a porous media, in an aquifer. In this chapter, we will give an introduction to the theory of two phase flow in a porous media. This theory is the foundation which we will build our mathematical model on in later chapters.

2.1 A porous media

A porous media consists of a solid material and empty space, pores as seen in Figure 2.1. The porosity of a porous media is defined as the fraction of pore volume, V_P over total volume or bulk volume, V_B,

$$\phi = \frac{V_P}{V_B}.$$

However, as seen in Figure 2.1, there might be isolated pores in our media, which do not contribute to the total flow through the system. We therefore define the effective pore volume, V_E as the volume of the connected pores, and the effective porosity,

$$\phi_E = \frac{V_E}{V_B}.$$

From now on, we will only say porosity, and write ϕ when we really mean the effective porosity. The porosity is a dimensionless parameter, and is a number between 0 and 1, but often expressed as a percentage. There are many different types of porous media. The one we will consider in this thesis is sandstone, a rock consisting of tiny grains of sand with empty space inbetween.

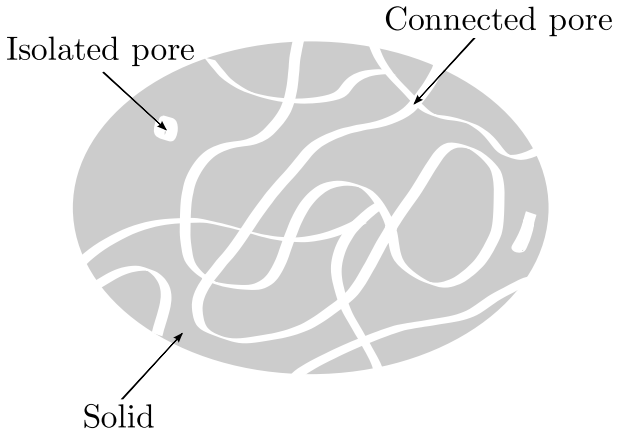

Figure 2.1: A porous media with solid material (grey) and a channel of pores (white)

REV and continuum assumption

In a porous media, the fluid flows in very irregular pores. In principal, we could use hydrodynamic laws to model the fluid flow in each individual pore. However, unless our porous media is of the very simplest kind, we do not know the geometry of the pores on micro scale. We therefore need to make a continuum assumption on macroscopic scale, so that we can average our properties, like the porosity, over a representative elementary volume (REV). Note that if we look at a volume small enough, the porosity will always be either 0 or 1 depending on whether we are in a pore or in the solid. REV is defined as the volume so that any smaller volume has large variations in properties like for instance porosity.

$$\text{Characteristic volume of the aquifer} \gg REV \gg \text{pore diameter}$$

Any volume greater than or equal to the REV is considered as a continuum with well defined macro scale properties.

2.1.1 Permeability

The permeability is a property of the porous media, and can be interpreted as the material's ability to lead fluid [*Pettersen*, 1990]. Generally, the permeability will be a second order tensor, $\mathbf{k}$, meaning that the permeability

can vary both with position (inhomogeneity) or with direction of fluid flow (anisotropy). The permeability is measured in Darcy, or milliDarcy, where 1 Darcy $= 9.869233 \cdot 10^{-13} m^2$ [*Pettersen*, 1990].

2.2 Fluid properties

The fluids also have some properties that are important for the behaviour of the system. We study a system of two phases, and let $\alpha = c, w$ denote the two phases CO_2 and salty water, or brine. Each fluid has a density defined as

$$\rho_\alpha = \frac{\text{mass of phase } \alpha}{\text{volume of phase } \alpha},$$

with units [kg/m^3]. The viscosity, μ_α, of a fluid tells us how well the fluid flows. The more viscous, the slower it flows. For instance, honey will be more viscous than water. The viscosity is measured in [Pa·s]. For brine, both the density and viscosity will depend on the salinity of the water. For CO_2, the density and viscosity will depend on the pressure and temperature. Figure 2.2 shows how the density of CO_2 depends on both temperature and pressure. For the rest of this thesis we will only look at the pressure dependence. This leads us to define the compressibility β of the CO_2 phase

$$\frac{1}{\rho_c}\frac{d\rho_c}{dp_c} = \beta, \tag{2.1}$$

which describes the relationship between the fluid pressure and the density, that is how the volume of the fluid changes as a cause of changes in pressure. The compressibility has the unit [1/Pa].

2.2.1 Wetting and nonwetting fluids

In a system of two fluids, one will always be the wetting phase and one the nonwetting phase. The wetting phase tends to cling more to the solid than the non-wetting phase. The wettability is determined by the contact angle between the fluid and the solid as shown in Figure 2.3.

$$\begin{array}{ll} \theta < \frac{\pi}{2} & \text{Wetting fluid} \\ \theta > \frac{\pi}{2} & \text{Nonwetting fluid} \end{array}$$

In our system, brine will be the wetting phase and CO_2 the nonwetting one. When a wetting fluid is injected into an aquifer, and displaces the nonwetting fluid, we call the displacement an imbibition process. When it is the other way around, the nonwetting fluid displaces the wetting fluid and we have a

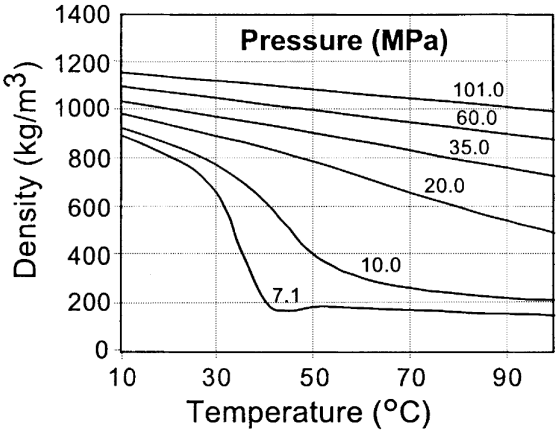

Figure 2.2: Density of CO_2 as a function of temperature and pressure, from *Bachu* [2002]

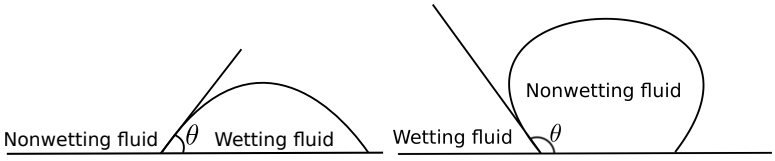

Figure 2.3: The wettability of a fluid is defined by the contact angle θ. The wetting fluid tends to cling more to the solid than the nonwetting one.

drainage process. In our case, we will then first have a drainage process as the CO_2 is injected into the aquifer and displaces the brine, and then as the CO_2 plume migrates upwards, we will have an imbibition process behind the plume, as brine again displaces the CO_2 , as illustrated in Figure 2.4.

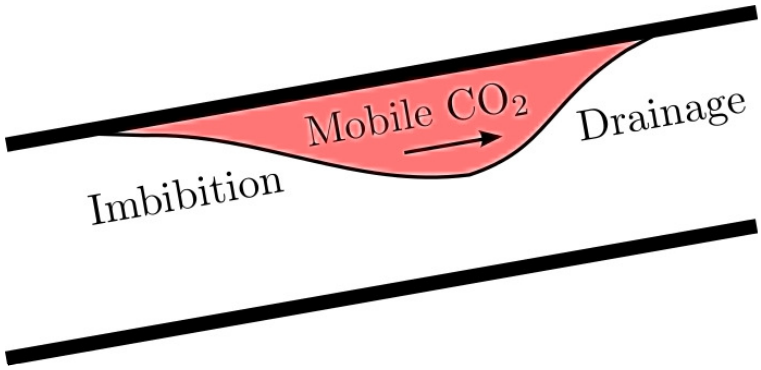

Figure 2.4: Drainage and imbibition in a CO_2 storage situation.

2.2.2 Saturation

For a multi-phase system, we say that the phase saturation is the fraction of the pore volume that consists of that phase,

$$s_\alpha = \frac{\text{volume of phase } \alpha}{\text{total effective pore volume}}.$$

All the pore space must always be filled with something, so that the sum of all the phase saturations will always be 1. In our case, this leads to the saturation balance equation

$$s_c + s_w = 1. \tag{2.2}$$

When we replace one fluid with another in a porous media, we will not be able to remove all the fluid. Some of the replaced fluid will always remain. The wetting phase, which clings to the solid, will remain in the porous media as a thin film around the solids, while the nonwetting phase will remain as small islands in the pores, see Figure 2.5. We call these minimal saturations s_{wr} for the wetting phase (brine), and s_{cr} for the nonwetting phase (CO_2).

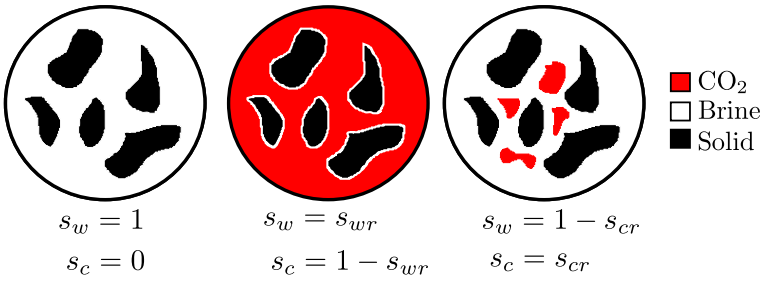

Figure 2.5: Residual saturation after drainage and imbibition. The left figure shows a porous media completely saturated with brine. In the middle figure, CO_2 has been injected and drained the brine from the medium, leaving only residual brine. As brine is imbibed back into the porous medium as shown in the right figure, there will only be immobile, residually trapped CO_2 left.

2.2.3 Pressure

Each fluid has its fluid pressure p_α. The pressure in the aquifer is hydrostatic from the surface and increasing as we go downwards as a function of the gravity and the density of the fluid above [*Celia and Nordbotten*, 2012].

$$p_{abs} = p_{atm} + \rho g(h - z) \tag{2.3}$$

In this thesis, we will look at the pressure relevant to some known reference pressure p_0, connected with a known CO_2 density ρ_0, so that our pressure distribution will be

$$p_\alpha = p_0 + \rho_\alpha g(h - z). \tag{2.4}$$

2.2.4 Relative permeability

When more than one fluid is present in the system, we also have to consider the relative permeability, which is a reduction in the materials permeability due to interaction with the other phases. The relative permeability, $k_{r\alpha}$, is a known, possible hysteretic, function of the saturation and is a dimensionless parameter between 0 and 1. There are many different models for the relative permeabilities.

2.3 Darcy's law

Darcy's law is an empirical law found by the French engineer Henry Darcy in the 1850s [*Pettersen*, 1990]. After experimenting on water flowing through a column of sand, he found that the filtration velocity, or Darcy-velocity, of the water is proportional to the pressure drop over the height. More experimenting, for instance with different types of fluids and sandstones with different permeabilities has led to a modern version of Darcy's law for two phase flow

$$\mathbf{u}_\alpha = -\lambda_\alpha \mathbf{k} \left(\nabla p_\alpha - \rho_\alpha \mathbf{g} \right), \tag{2.5}$$

where $\alpha = c, w$ denotes the two phases. In this equation, p_α stands for the fluid pressure, $\mathbf{g}$ is the gravity vector and λ_α stands for mobility of phase α, where $\lambda_\alpha = \frac{k_{r\alpha}}{\mu_\alpha}$. This means that the mobility has units [1/Pa·s]

2.4 Mass conservation

The other fundamental equation we will look at is the mass conservation equation. The mass conservation equation is based on the simple fact that the mass is conserved, so that what is accumulated in a cell, is the same as what flows into the same cell minus what flows out.

$$\{\text{Rate of change of mass}\} + \{\text{Rate of outflow}\} = 0.$$

Writing this in mathematical terms, we look at the cell defined in Figure 2.6. What is accumulated in this cell, is the time derivative of the total mass inside the domain, which we get by integrating the mass over the interval

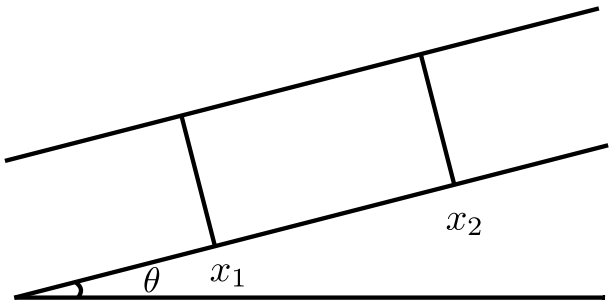

Figure 2.6: Integration domain used to derive the mass conservation equation

$[x_1, x_2]$. The second term, what flows in and out, is simply the density times the Darcy velocity evaluated at the two boundaries x_1 and x_2. Putting all this together, we get our mass conservation equation on integral form

$$\frac{\partial}{\partial t}\int_{x_1}^{x_2} \phi s_\alpha \rho_\alpha \mathrm{d}x + [\rho_\alpha u_\alpha]_{x_1}^{x_2} = 0.$$

Using the divergence theorem, we can rewrite the last term of this mass conservation equation to an integral. Further, with the use of Leibniz integral rule, we can move the time derivative inside the integral. We now have an integral over an arbitrary interval that is zero, which means that also the integrand needs to be zero, and we get our mass conservation equation on differential form

$$\frac{\partial}{\partial t}\left(\phi \rho_\alpha s_\alpha\right) + \frac{\partial}{\partial x}\left(\rho_\alpha u_\alpha\right) = 0. \tag{2.6}$$

2.5 Spatial and temporal scales

As we briefly mentioned in Chapter 1, we are interested in knowing something about which scales important processes take place. First, lets look at some spatial scale issues. The spatial scales ranges from the smallest fluid interfaces on micro scale to the largest spatial scale of interest, the horizontal extent of the aquifer. The micro scale may be around 10^{-6}m while the macro scale is about 10^5m (some hundred kilometres). This gives us a spatial scale ratio of 10^{11} [*Celia and Nordbotten*, 2012]. Looking at the temporal scales, one important thing to consider is the regulatory framework. There are expectations of how long the injection should go on, usually for about 50 years, and also guidelines for the long term fate of the CO_2. How long does the CO_2 have to stay in the aquifer for the storage operation to be considered as a success? And how much leakage can we accept for how long? These are important questions on the macro temporal scale. Another important

feature is how long time it will take before we have density segregation, which according to *Celia and Nordbotten* [2012] takes about a year. This is important because it is only after this that our VE model, which will be described more in the next chapter, is valid.

Chapter 3

Mathematical model

In this chapter, we derive upscaled analogous to the fine scale equations stated in the previous chapter. We will then derive one equation for the pressure, and sketch a method for solving the equations.

3.1 Approximations

Before we start looking at our equations, we need to state the assumptions we will use in our further work.

We consider a 2D aquifer as a porous media with length L and uniform thickness H, tilted with an angle θ. Above and below the aquifer there are impermeable layers, also called caprocks, see Figure 3.1. We assume that the aquifer is uniform, which means that it is both homogeneous and isotropic. The permeability tensor $\mathbf{k}$ will then only be a constant scalar, k. We also assume that the matrix is incompressible and that the conditions are isothermal.

We assume that we have only two fluids, CO_2 and salty water, brine, flowing. The aquifer is initially filled with brine, which will be displaced by CO_2 in a drainage process. The fluids are immiscible, and separated by a sharp interface. Below this interface, there will be pure brine, which means that the brine saturation $s_w = 1$, and the saturation of CO_2 , $s_c = 0$. Above the interface, there will be some residual brine trapped as described in Section 2.2.2. We will then have a brine saturation equal to the residual wetting phase saturation $s_w = s_{wr}$, and the CO_2 saturation will be $s_c = 1 - s_{wr}$. This gives us the following saturation distribution

$$s_c = \begin{cases} 0 & \text{if } 0 \leq z < h \\ 1 - s_{wr} & \text{if } h \leq z < H \end{cases}$$

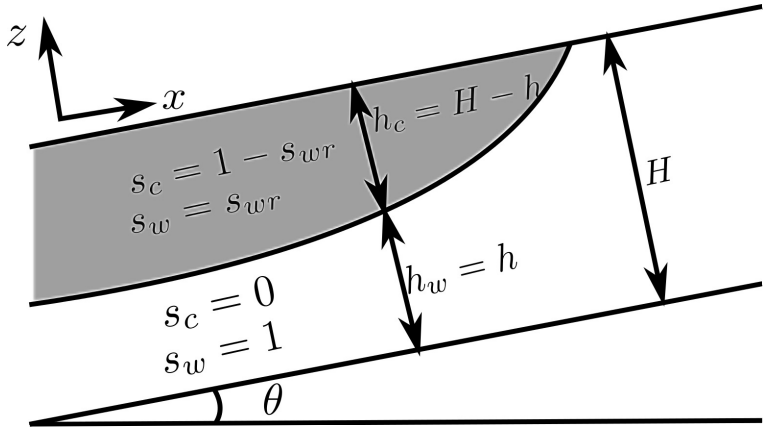

Figure 3.1: Aquifer

$$s_w = \begin{cases} 1 & \text{if } 0 \leq z < h \\ s_{wr} & \text{if } h \leq z < H. \end{cases}$$

We also assume that brine is incompressible, while CO_2 is compressible with a constant compressibility β. We assume that the aquifer is deep enough so that the CO_2 is supercritical, which for typical geothermal gradients of about 30°C/km and a surface temperature of about 25°C means deeper than about 800 meters [*Celia and Nordbotten*, 2012].

We also assume that we have **vertical equilibrium** which is a condition where the sum of all the fluid flow driving forces in the direction perpendicular to the direction of bulk fluid flow is zero [*Lake*, 1989]. We denote L as the characteristic aerial extent, and H as the uniform thickness of the aquifer. The reservoir we are considering has a typical length scale of some kilometres while the thickness, H, has magnitude of some tens of meters. If we also have a suitable permeability ratio $\delta_K = \dfrac{k_z}{k_H}$ such that $L \gg \sqrt{\delta_K} H$, where k_z is the vertical permeability and k_H the horizontal permeability, the vertical equilibrium model is a reasonable approximation.

3.2 Multiscale modelling

With the different scales described in Section 2.5 in mind, we want to use a multiscale approach to solve our problem. To decrease the computational effort, we resolve the problem on macro scale. However, due to the high

ratio between the lateral and vertical extent, the vertical length scale will not be resolved in this model. We therefore use a vertical integration model, where we integrate the equations over the z-axis. Our 3D models will then be upscaled to 2D models. Figure 3.2 illustrates the solution procedure for

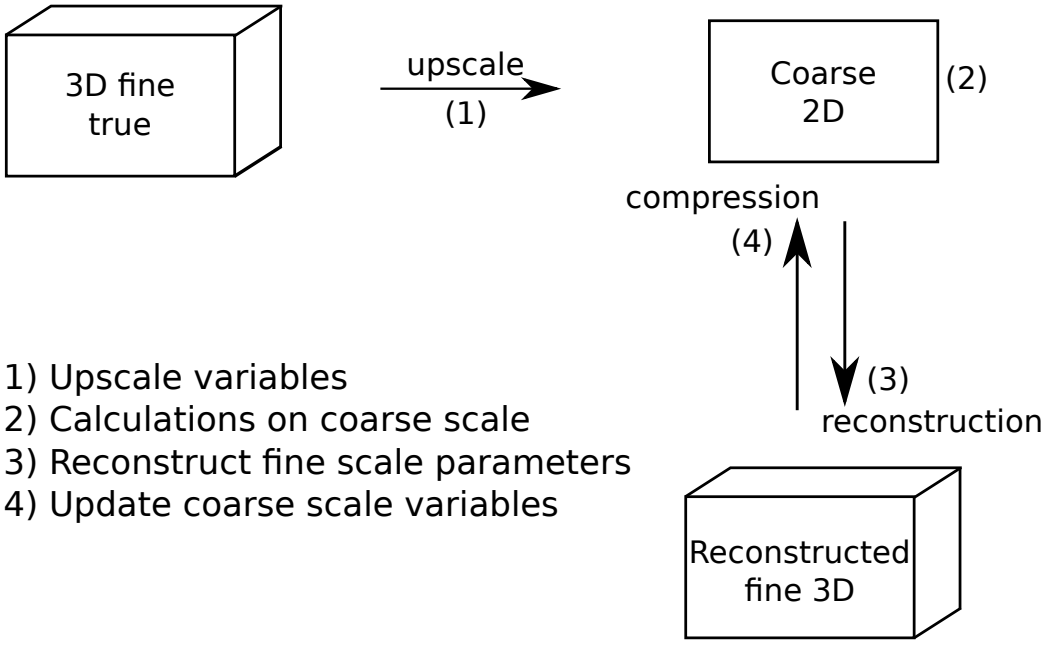

Figure 3.2: Illustration of solution procedure using multiscale modelling.

a multiscale model approach. First, we upscale our equations by integrating them over the z-axis (1). Since we start out with 2D equations, our upscaled equations will be 1D, which will significantly decrease the computational effort. These coarse scale equations can now be solved on the coarse scale (2). We can then reconstruct the saturation distribution on a reconstructed fine scale using the assumptions of sharp interface and Vertical Equilibrium (3). Then, we use this reconstructed saturation to update our coarse scale variables (4), before we solve the equations once more on the coarse scale. This loop is repeated for each time step, until we have run the simulation as long as desired.

3.3 Pressure profile

We now want to derive an expression for the coarse scale pressure. We simply choose this pressure to be the pressure at the interface h, such that $P_\alpha(x, y) = p_\alpha(x, y, z = h)$. We also assume that there is no pressure difference on the

CO_2-brine interface, so that $P_c = P_w$. Because of the vertical equilibrium assumption, the vertical velocity is negligible compared to the horizontal: $\|\mathbf{u}_\alpha^H\| \gg u_\alpha^z$. Inserting this assumption into Darcy's law (2.5), we get

$$u_\alpha^z = -\lambda_\alpha k_z \left(\frac{dp_\alpha}{dz} + \rho_\alpha g_z \right) = 0, \tag{3.1}$$

which leads to

$$\frac{dp_\alpha}{dz} = -\rho_\alpha g \cos\theta. \tag{3.2}$$

For brine, which we assume to be incompressible, we can simply integrate this equation from the height of the interface, $z = h$, to an arbitrary height, z, to obtain an equation relating the coarse and the fine scale pressure

$$p_w = P - \rho_w g \cos\theta \, (z - h). \tag{3.3}$$

3.3.1 CO_2 density and pressure

Since the density of CO_2 is dependent on z, we can not simply integrate to obtain a similar pressure equation for CO_2. First, we will use the Equation Of State (EOS) (2.1) to derive an analytic expression for the density of CO_2. Then we will linearise the density to obtain a linearised function for the pressure of CO_2.

We start out with our EOS (2.1). Integrating this, we see that the density varies exponentially with pressure.

$$\rho_c = \rho_0 e^{\beta(p_c - p_0)}. \tag{3.4}$$

Equation (3.4) describes how the density vary with pressure. However, the pressure varies with the vertical coordinate in the aquifer, z, and what we want is to have an equation where the density varies explicitly with the z-coordinate. To obtain this, we go back to our pressure equation (3.2) and combine it with our original EOS (2.1). Integrating this equation from the CO_2-brine interface, $z = h$, to an arbitrary height, z, we get

$$-\frac{1}{\rho_c(z)} + \frac{1}{\rho_c(h)} = -\beta g \cos\theta \, (z - h). \tag{3.5}$$

Evaluating Equation (3.4) at $z = h$ and inserting it into (3.5) we get

$$\rho_c(z) = \frac{\rho_0}{e^{-\beta(P - p_0)} + \rho_0 \beta g \cos\theta \, (z - h)}. \tag{3.6}$$

We now have an analytical expression for ρ_c as a function of z. Figure 3.3 shows this relationship for different values of the compressibility β when $\theta = 0$ and the reference pressure and density are measured at the uniform interface at height h.

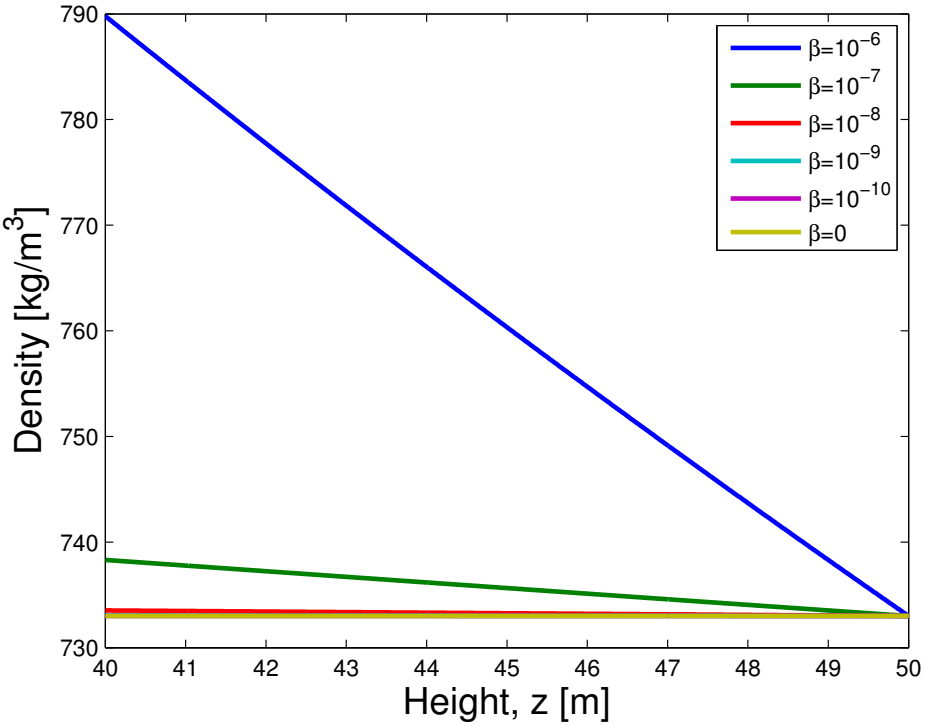

Figure 3.3: Density as a function of height, plotted for different values of the compressibility β, where $\rho_0 = 733\text{kg/m}^3$ and $\theta = 0$.

3.3.2 Linearisation of density

We now want to obtain an expression for the pressure of CO_2, similar to Equation (3.3) for brine. Based on the Taylor expansion of the exponential function we can linearise the density expression (3.4)

$$\rho_c = \rho_0 e^{\beta(p_c - p_0)} \approx \rho_0 \left(1 + \beta \left(p_c - p_0\right)\right). \tag{3.7}$$

Inserting this into Darcy's law for CO_2, with the vertical equilibrium assumption (3.2), we get the differential equation describing the pressure as a function of the density

$$\frac{\partial p_c}{\partial z} = -\rho_c g \cos\theta = -G\left(1 + \beta\left(p_c - p_0\right)\right) \tag{3.8}$$

where $G = \rho_0 g \cos\theta$. Integrating from h to z, and linearising the exponential term, we get the following linear reconstruction of the CO_2 pressure

$$p_c(z) = P - G\left(z - h\right)\left(1 + \beta\left(P - p_0\right)\right). \tag{3.9}$$

We now have linear approximations for both the density (3.7) and the pressure of CO_2 (3.9). Combining these two equations, we get an expression for the density as a function of z

$$\rho_c(z) = a(h, P) + b(P)z \tag{3.10}$$

where

$$\begin{aligned} a(h, P) &= \rho_0 + \rho_0\beta(P - p_0) + \rho_0\beta G h + \rho_0\beta^2 G(P - p_0)h \\ b(P) &= -\rho_0\beta G - \rho_0\beta^2 G(P - p_0). \end{aligned}$$

This linearised expression for the density is a substitute for (3.6). Calculating the difference between the true density and the linearised density, for a test case of $h = 50$m, over an aquifer from $z = 40$m to $z = 50$m, we get that the max norm of this error is less than $4 \cdot 10^{-4}\text{kg/m}^3$, which relative to the density is at the order of 10^{-7}, which is a very small error.

3.4 Upscaled equations

As described in Section 3.2, we now want to derive coarse scale analogous to the governing equations described in the previous chapter. Following the procedure from e.g. *Nordbotten and Dahle* [2011], we integrate our equations over the z-axis of our aquifer. In the following derivation, lower case letters denote parameters on the fine scale while upper case letters denote upscaled, coarse scale parameters.

3.4.1 Mass conservation equation

We start out with our fine scale mass conservation for CO_2

$$\frac{\partial}{\partial t}(\phi\rho_c s_c) + \frac{\partial}{\partial x}(\rho_c u_c) = 0. \tag{3.11}$$

We define upscaled porosity as $\Phi = \frac{1}{H}\int_0^H \phi \, \mathrm{d}z$. However, the porosity is assumed to be constant, so this reduces to $\Phi = \phi$. Further, we define the upscaled saturation and density as

$$S_c = \frac{1}{H}\int_0^H s_c \, \mathrm{d}z, \qquad R_c = \frac{\frac{1}{H}\int_0^H (\rho_c s_c) \, \mathrm{d}z}{S_c}. \tag{3.12}$$

If we assume that the fluids are segregated by a sharp interface, like in Figure 3.1, the upscaled saturation and density for the CO_2 phase becomes

$$S_c = \frac{H-h}{H}\left(1 - s_{wr}\right), \qquad R_c = \frac{1}{h_c}\int_{h_c} \rho_c \, \mathrm{d}z. \tag{3.13}$$

With these definitions, we can integrate (3.11) over the z-axis of our aquifer and get a coarse mass conservation equation for CO_2

$$\Phi \frac{\partial}{\partial t}\left(R_c S_c\right) + \frac{\partial}{\partial x} F_{M_c} = 0 \tag{3.14}$$

where the mass flux is defined as

$$F_{M_c} = \frac{1}{H}\int_0^H \rho_c u_c \, \mathrm{d}z. \tag{3.15}$$

For the brine phase, we do the exact same integration procedure. However, since brine is incompressible, the density ρ_w is constant and can be moved outside the time differential. We keep the fine scale notation on this constant density

$$\Phi \rho_w \frac{\partial S_w}{\partial t} + \frac{\partial}{\partial x} F_{M_w} = 0. \tag{3.16}$$

We now have our two upscaled mass conservation equations. These have exactly the same form as their fine scale analogous (2.6), and the only difference is the interpretation of the coarse scale variables vs. the fine scale variables.

3.4.2 Darcy's law

We now proceed to the upscaling of the second governing equation described in Chapter 2, Darcy's law. We start out with the fine scale version of Darcy's law for CO_2

$$u_c = -\lambda_c k \left(\frac{\partial p_c}{\partial x} - \rho_c g \sin\theta\right). \tag{3.17}$$

We define the upscaled mobility and permeability as

$$K = \frac{1}{H}\int_0^H k \mathrm{d}z = k \tag{3.18}$$

$$\Lambda_c = \lambda_c^r \cdot \left(1 - \frac{h}{H}\right) \tag{3.19}$$

where the mobility is given by $\lambda_c^r = \frac{k_{rc}(s_c = 1 - s_{wr})}{\mu_c}$

We insert the linearised pressure equation (3.9) into Darcy's law (3.17) and multiply with ρ_c. We then follow the same procedure as for the mass conservation equations, and integrate from 0 to H. Using the following definitions of density and the square density

$$R_c = \frac{\frac{1}{H}\int_0^H \lambda_c k \rho_c \frac{\partial P}{\partial x}\,\mathrm{d}z}{\Lambda_c K \frac{\partial P}{\partial x}} = \frac{1}{h_c}\int_{h_c} \rho_c\,\mathrm{d}z \tag{3.20}$$

$$\hat{R}_c^2 = \frac{\frac{1}{H}\int_0^H \lambda_c k \rho_c^2\,\mathrm{d}z}{K\Lambda_c} = \frac{1}{h_c}\int_{h_c} \rho_c^2\,\mathrm{d}z. \tag{3.21}$$

and the definition of the mass flux F_{M_c} (3.15) we get the upscaled Darcy's law for CO_2

$$\begin{aligned} F_{M_c} = &- \Lambda_c K R_c \frac{\partial P}{\partial x} \\ &+ \Lambda_c K \frac{\partial P}{\partial x} \beta G \left[\frac{1}{2}a\left(H+h\right) + \frac{1}{3}b\left(H^2 + Hh + h^2\right) - hR_c\right] \\ &- \frac{\partial h}{\partial x} G\left(1 + \beta\left(P - p_0\right)\right)\Lambda_c K R_c \\ &+ \Lambda_c K \hat{R}_c^2 g \sin\theta. \end{aligned} \tag{3.22}$$

With the use of our equation for density as a function of z (3.10), we can write out the upscaled density and the upscaled square density, R_c and $\hat{R}_c^2$, as equations varying explicitly on h and P for use in the further derivation

$$\begin{aligned} R_c &= a + \frac{1}{2}b\left(H+h\right) \\ \hat{R}_c^2 &= a^2 + ab\left(H+h\right) + \frac{1}{3}b^2\left(H^2 + Hh + h^2\right). \end{aligned}$$

We can now use this same procedure to upscale Darcy's law for the brine phase. We start out with the fine scale version of Darcy's law, and insert the pressure equation (3.3)

$$u_w = -\lambda_w k\left(\frac{\partial P}{\partial x} + \rho_w g\cos\theta\frac{\partial h}{\partial x} - \rho_w g\sin\theta\right). \tag{3.23}$$

We define the upscaled mobility for brine as

$$\Lambda_w\left(s_w\right) = \lambda_w^r \cdot \left(\frac{h}{H}\right) \tag{3.24}$$

where the residual mobility is given by $\lambda_w^r = \frac{k_{rw}(s_{cr})}{\mu_w}$. We then multiply Equation (3.23) with ρ_w and integrate from 0 to H to get the upscaled Darcy's law for brine

$$F_{M_w} = -\Lambda_w K \rho_w \left(\frac{\partial P}{\partial x} + \rho_w g \cos\theta \frac{\partial h}{\partial x} - \rho_w g \sin\theta \right). \tag{3.25}$$

We see that this equation has very much the same form as its fine scale analogue (2.5), only with different interpretation of the coarse scale variables compared to the fine scale ones. The equivalent equation for CO_2 looks very different from its fine scale analogue, due to a mess made by the compressibility. However, if we set $\beta = 0$, we are back at the incompressible case, and Equation (3.22) looks exactly like Equation (3.25).

3.5 Pressure equation

We now want to use these upscaled equations to derive one equation for the coarse scale pressure. We write out the upscaled mass conservation equation for CO_2 (3.14) and for brine (3.25) using the product rule and divide by R_c and ρ_w respectively. We then add the two equation to obtain

$$\Phi \left(\underbrace{\frac{\partial S_c}{\partial t} + \frac{\partial S_w}{\partial t}}_{=0} + \frac{S_c}{R_c}\frac{\partial R_c}{\partial t} \right) + \frac{1}{R_c}\frac{\partial}{\partial x} F_{M_c} + \frac{1}{\rho_w}\frac{\partial}{\partial x} F_{M_w} = 0 \tag{3.26}$$

To incorporate the compressibility explicitly, we rewrite the time derivative of the density in terms of compressibility

$$\frac{1}{R_c}\frac{\partial R_c}{\partial t} = \left(\frac{1}{R_c}\frac{\partial R_c}{\partial P} \right) \frac{\partial P}{\partial t} = \beta^* \frac{\partial P}{\partial t}.$$

The parameter β^* is not the same as the compressibility value β, but is some kind of upscaled pseudo compressibility. Written out, this parameter looks like

$$\beta^* = \frac{1}{R_c}\left(\rho_0 \beta - \rho_0 \beta^2 G h + \frac{1}{2}\rho_0 \beta^2 G \left(H + h \right) \right),$$

so we see that β^* is zero when β is.

Inserting this definition into (3.26) we get a pressure equation

$$\Phi S_c \beta^* \frac{\partial P}{\partial t} + \frac{1}{R_c}\frac{\partial}{\partial x} F_{M_c} + \frac{1}{\rho_w}\frac{\partial}{\partial x} F_{M_w} = 0.$$

We can then substitute the fluxes in this equation using the upscaled Darcy's laws (3.22) and (3.25) and we are left with

$$A\frac{\partial P}{\partial t} - \frac{1}{R_c}\frac{\partial}{\partial x}\left[B\frac{\partial P}{\partial x} - C\right] - \frac{\partial}{\partial x}\left[D\frac{\partial P}{\partial x} - E\right] = 0 \tag{3.27}$$

where

$$\begin{aligned}
A(h) &= \Phi S_c \beta^* = \phi\frac{H-h}{H}(1-s_{wr})\beta^* \\
B(h,P) &= \Lambda_c K R_c - \Lambda_c K \beta G\left(\frac{1}{2}a\left(H+h\right) + \frac{1}{3}b\left(H^2+Hh+h^2\right) - hR_c\right) \\
C\left(h,P\right) &= -\Lambda_c K R_c G\left(1+\beta\left(P-p_0\right)\right)\frac{\partial h}{\partial x} + \Lambda_c K \hat{R}_c^2 g\sin\theta \\
D(h) &= \Lambda_w K \\
E(h) &= -\Lambda_w K g \rho_w\left(\cos\theta\frac{\partial h}{\partial x} - \sin\theta\right).
\end{aligned}$$

3.6 Discussion

Equation (3.27) is based on the equations describing the conservation of mass within the system. Grouping the terms in the equation the way we have done, we see that this equation has the structure of a conservation equation. The A-term is a pressure accumulation term that allows us to have accumulation of pressure within a cell due to compressibility. This term is similar to the terms we find in work including horizontal compressibility, like the paper by *Gasda et al.* [2009]. The difference from our pressure equation compared to these works, is that we also have compressibility in the other terms, giving us terms expressing transport of pressure.

We have thus incorporated the compressibility in two different ways. The first is the horizontal compressibility, which we get by writing out the $\frac{\partial(\rho_c s_c)}{\partial t}$-term explicitly in the mass conservation equation. This gives us the compressibility in the accumulation term A in Equation (3.27). The second is to include vertical dependence in ρ_c in the pressure equation (3.2). This gives us the vertical compressibility that we see in the B- and C-terms in Equation (3.27).

Including vertical compressibility the way we have done it gives us an extra nonlinearity in the equation, that rises some extra challenges on how to discretise the equation. We will look more at this in the next chapter.

The B- and C-term are related to the CO_2 phase, while the D- and E-terms are strictly related to the brine phase and does not depend on the pressure. The C-term is a hyperbolic transport part, while the D-term is a parabolic diffusion term. Note that if we set $\beta = 0$, that is, we make the system incompressible, the A-term disappears, and the B- and C-terms will be exactly the same as the D- and E-terms, and no longer depend on the pressure. The equations we get then, we recognise from other works on incompressible flow, like in the paper by *Nordbotten and Dahle* [2011].

Chapter 4

Numerical model

In this chapter, we will summarize the equations derived in the previous chapter, and sketch a procedure for solving the problem. We will then derive discrete analogous to these differential equations that we can solve numerically. To do this, we also need to look at some theory from numerics.

4.1 Solution approach

We want to solve our equations with an IMPES (IMplicit Pressure Explicit Saturation) method. The basic idea of an IMPES-method is to solve a coupled system of partial differential equations by separating the computation. First, we solve the pressure equation implicitly, but with coefficients from the previous time step, and then solve the saturation equation explicitly [*Chen et al.*, 2004]. The solution procedure can be summarized in the steps below.

1. Setting initial conditions

   - h^0
   - P^0
   - Mass fluxes

2. Solving our pressure equation

$$A\frac{\partial P}{\partial t} - \frac{1}{R_c}\frac{\partial}{\partial x}\left[B\frac{\partial P}{\partial x} - C\right] - \frac{\partial}{\partial x}\left[D\frac{\partial P}{\partial x} - E\right] = 0 \qquad (4.1)$$

3. Calculate the mass fluxes using Darcy's laws for CO_2 and brine

$$\begin{aligned} F_{M_c} =& -\Lambda_c K R_c \frac{\partial P}{\partial x} \\ &+ \Lambda_c K \frac{\partial P}{\partial x} \beta G \left[\frac{1}{2} a \left(H + h \right) + \frac{1}{3} b \left(H^2 + Hh + h^2 \right) - h R_c \right] \\ &- \frac{\partial h}{\partial x} \left(G \left(1 + \beta \left(P - p_0 \right) \right) \right) \Lambda_c K R_c \\ &+ \Lambda_c K \hat{R}_c^2 g \sin\theta \end{aligned} \tag{4.2}$$

$$F_{M_w} = -\Lambda_w K \rho_w \left(\frac{\partial P}{\partial x} + \rho_w g \cos\theta \frac{\partial h}{\partial x} - \rho_w g \sin\theta \right) \tag{4.3}$$

4. Update the masses in each cell using the mass conservation equations

$$\Phi \frac{\partial M_c}{\partial t} + \frac{\partial}{\partial x} F_{M_c} = 0 \tag{4.4}$$

$$\Phi \frac{\partial M_w}{\partial t} + \frac{\partial}{\partial x} F_{M_w} = 0 \tag{4.5}$$

5. Calculate the saturations/height of the interface using the mass of brine or the mass of CO_2

$$M_c = R_c(h, P) S_c(h) = R_c(h, P) \frac{H - h}{H} \left(1 - s_{wr} \right) \tag{4.6}$$

$$M_b = \rho_b S_b(h) = \rho_b \left(\frac{h}{H} + \frac{H - h}{H} s_{wr} \right) \tag{4.7}$$

4.2 Numerical approach

To solve the partial differential equations in Section 4.1, we need to discretise them into difference equations and solve them numerically. This discretisation become somewhat more challenging than for the incompressible case, since the compressibility introduces more nonlinearity to the problem, and also because first order transport terms needs to be addressed. We also have to consider which terms to have explicit and which terms to have implicit in our discretisation.

Equation (4.1) consists of both a hyperbolic term (C) and a parabolic term (B), in addition to the terms that does not depend P (D,E). To discretise these, we need to use appropriate methods for both terms. For the parabolic term, which contain a second order derivative, we simply integrate the equation over a control volume to obtain a difference equation, and solve

this implicitly. For the hyperbolic term, we have to be careful when we choose a discretisation method. One common procedure for hyperbolic conservation laws in is to use upstream weighting for the hyperbolic terms. However, this equation describes the pressure transport, and pressure does not flow upstream in the way that for instance water does. In this thesis, we have chosen to use the Lax-Friedrichs' method on the hyperbolic transport terms.

4.2.1 Control volume method

We remember from Section 2.4 that the mass balance equation, which our pressure equation is based on, was originally an integral equation. Instead of deriving a numerical approximation directly from (3.27), we now want to return to our original integral formulation, to make sure that we preserve the conservation originally expressed. We start out by dividing our domain into an equidistant grid, and denote our cell centre nodes x_i. The left and right boundary are denoted x_L and x_R respectively. Each cell is separated from the two neighbouring by an interface $x_{i-1/2}$ as shown in Figure 4.1. We also

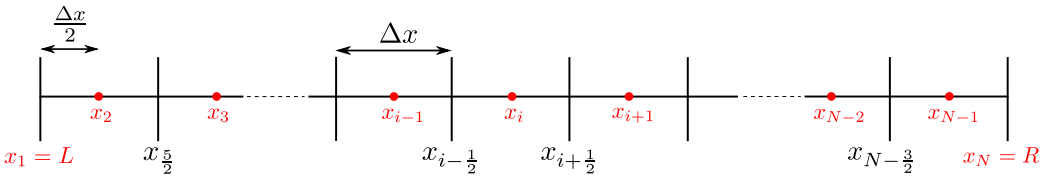

Figure 4.1: Domain divided in a grid

have to integrate our equation in time. We divide our continuous time into discrete time levels t^j, $j = 0, 1, ..., n$ where t^0 denotes our initial condition. We now integrate our pressure equation (3.27) over a control volume Ω as shown in Figure 4.2

$$\iint_\Omega A\frac{\partial P}{\partial t}\mathrm{d}t\mathrm{d}x - \iint_\Omega \frac{1}{R_c}\frac{\partial}{\partial x}\left(B\frac{\partial P}{\partial x} - C\right)\mathrm{d}x\mathrm{d}t - \iint_\Omega \frac{\partial}{\partial x}\left(D\frac{\partial P}{\partial x} - E\right)\mathrm{d}x\mathrm{d}t = 0.$$

We start by setting averaged values of A and R_c outside of the integrals. We denote these values $\overline{A}$ and $\overline{R_c}$ and they are then averages of A and R_c over the control volume Ω, that is, both over the time interval $[t^n, t^{n+1}]$ and over the space interval $\left[x_{i-1/2}, x_{i+1/2}\right]$. In the following, we will use $\overline{R_c} = R_c(x_i)^n$ and $\overline{A} = A(x_i)^n$.

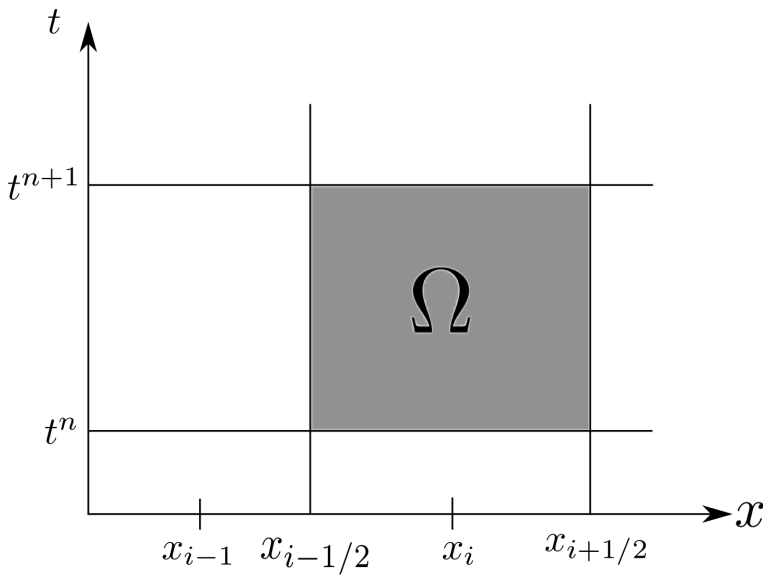

Figure 4.2: Integration domain Ω

Now we can use the Fundamental Theorem of Calculus to remove one of the integrals against one the x- or t-derivatives, and the values inside simply gets evaluated at the endpoints of the integral. We can now evaluate the integrals and get our discrete difference equation based on this control volume method

$$\begin{aligned}\overline{A}\left(P_i^{n+1}-P_i^n\right) &- \frac{\Delta t}{\Delta x\overline{R_c}}\Big[\left(B_{i+1/2}^n\frac{P_{i+1}^{n+1}-P_i^{n+1}}{\Delta x}-C_{i+1/2}\right)\\ &-\left(B_{i-1/2}^n\frac{P_i^{n+1}-P_{i-1}^{n+1}}{\Delta x}-C_{i-1/2}\right)\Big]\\ &-\frac{\Delta t}{\Delta x}\Big[\left(D_{i+1/2}^n\frac{P_{i+1}^{n+1}-P_i^{n+1}}{\Delta x}-E_{i+1/2}\right)\\ &-\left(D_{i-1/2}^n\frac{P_i^{n+1}-P_{i-1}^{n+1}}{\Delta x}-E_{i-1/2}\right)\Big]=0.\end{aligned}$$

Note that we have estimated the derivatives implicitly for the parabolic part of the system. To estimate the coefficients B and D at the cell boundaries, we use harmonic averages of the values at the two neighbouring cell centres.

The question now is what about the two other coefficients, C and E. We know that these make up a hyperbolic part of the pressure equation, and we know then that we need to be careful about how to discretise them. Before we move on, we will therefore look at some theory regarding discretisation of hyperbolic conservation laws using the Lax-Friedrichs' method.

4.2.2 Lax-Friedrichs' method

Lax-Friedrichs' method is a method for solving hyperbolic conservation laws on the form

$$u_t + f(u)_x = 0. \tag{4.8}$$

The method is a central difference method, and looks like

$$u_i^{n+1} - \frac{1}{2}\left(u_{i-1}^n + u_{i+1}^n\right) + \frac{\Delta t}{2\Delta x}\left[f\left(u_{i+1}^n\right) - f\left(u_{i-1}^n\right)\right] = 0. \tag{4.9}$$

Defining the Lax-Friedrichs flux as

$$\phi^{LF}(u_L, u_R) = \frac{1}{2}\left[f(u_L) + f(u_R) - \frac{\Delta x}{\Delta t}\left(u_R - u_L\right)\right] \tag{4.10}$$

[*LeVeque*, 1992], this method can be rewritten as

$$\frac{u_i^{n+1} - u_i^n}{\Delta t} + \frac{\phi^{LF}\left(u_i^n, u_{i+1}^n\right) - \phi^{LF}\left(u_{i-1}^n, u_i^n\right)}{\Delta x} = 0. \tag{4.11}$$

In our pressure equation (4.1), the C-function represents the hyperbolic parts of the equation. We will therefore choose to rewrite the discretisation to a Lax-Friedrichs' type of discretisation for this part. The E-function also has a hyperbolic form, but E does not depend on P, which means that this will be a constant term. We choose to also represent the E-term in a Lax-Friedrichs' manner, but here we do not have to be as careful as we do with C, where we have to take special care to get the fluxes right on the boundaries. The red parts of the equation are the ones that have changed as we use Lax-Friedrichs' method

$$\begin{aligned}
&\overline{A}\left(P_i^{n+1} - P_i^n\right) \\
&-\frac{\Delta t}{\Delta x \overline{R_c}}\left[\left(B_{i+1/2}^n \frac{P_{i+1}^{n+1} - P_i^{n+1}}{\Delta x}\right) - \left(B_{i-1/2}^n \frac{P_i^{n+1} - P_{i-1}^{n+1}}{\Delta x}\right)\right] \\
&-\frac{\Delta t}{\Delta x}\left[\left(D_{i+1/2}^n \frac{P_{i+1}^{n+1} - P_i^{n+1}}{\Delta x}\right) - \left(D_{i-1/2}^n \frac{P_i^{n+1} - P_{i-1}^{n+1}}{\Delta x}\right)\right] \\
&+\frac{\Delta t}{\Delta x \overline{R_c}}\left(\Phi^{LF}(P_i^n, P_{i+1}^n) - \Phi^{LF}(P_{i-1}^n, P_i^n)\right) + \frac{\Delta t}{2\Delta x}\left(E_{i+1} - E_{i-1}\right) = 0.
\end{aligned}$$

For the internal nodes, we can write out our Lax-Friedrichs' flux expressions, to get back to the method on the form of Equation (4.9). However, we still have one more issue to address here. We have now discretised the hyperbolic part explicitly, not implicitly like the parabolic part, which should be fine,

since Lax-Friedrichs' method is stable under the CFL-condition even done explicitly. However, looking back at how we defined the C-function from Chapter 3, we see that there is a hidden second order derivative in this function, which can cause some problems. We therefore choose to do the C-term partially implicit, by dividing the C-function into
$C(h,P) = C1(h) + C2(h)\cdot P + C3(h)\cdot P^2$, and doing parts of it implicitly. Doing this, and gathering the terms, we then get our final difference equation for internal nodes $i = 3, ..., N-2$

$$\begin{aligned}
&P_i^{n+1}\left(\overline{A} + \frac{\Delta t}{\overline{R_c}\Delta x^2}\left(B_{i+1/2}^n + B_{i-1/2}^n\right) + \frac{\Delta t}{\Delta x^2}\left(D_{i+1/2} + D_{i-1/2}\right)\right) \quad (4.12)\\
&+P_{i+1}^{n+1}\left(-\frac{\Delta t}{\overline{R_c}\Delta x^2}B_{i+1/2}^n - \frac{\Delta t}{\Delta x^2}D_{i+1/2} + \frac{\Delta t}{2\Delta x\overline{R_c}}\left(C2_{i+1}^n + C3_{i+1}^n P_{i+1}^n\right)\right)\\
&+P_{i-1}^{n+1}\left(-\frac{\Delta t}{\overline{R_c}\Delta x^2}B_{i-1/2}^n - \frac{\Delta t}{\Delta x^2}D_{i-1/2} - \frac{\Delta t}{2\Delta x\overline{R_c}}\left(C2_{i-1}^n + C3_{i-1}^n P_{i-1}^n\right)\right)\\
&=\frac{1}{2}\overline{A}\left(P_{i-1}^n + P_{i+1}^n\right) - \frac{\Delta t}{2\Delta x\overline{R_c}}\left(C1_{i+1}^n - C1_{i-1}^n\right) - \frac{\Delta t}{2\Delta x}\left(E_{i+1} - E_{i-1}\right)
\end{aligned}$$

which can be written on matrix form

$$\mathbf{M}\mathbf{p}^{n+1} = \mathbf{y}^n \quad (4.13)$$

where the matrix $\mathbf{M}$ is a tridiagonal matrix and the right hand side vector $\mathbf{y}$ contains the functions $C1$ and E in addition to P^n.

4.2.3 Boundary

At the boundary, we have to write out the flux terms so that it fits with our discretisation shown in Figure 4.1. At the left boundary, we will take the left flux $\Phi_{3/2}^{LF} = C_1$, while the right flux will be estimated the same way as in the internal nodes. At the right boundary, we will take the right flux $\Phi_{N-1/2}^{LF} = C_N$, while the left flux will be estimated the same way as the internal fluxes. We also have to remember that the Δx distance from the discretisation of $\frac{\partial P}{\partial x}$ at the boundary, will now only be $\Delta x/2$. We then get

the following boundary term discretisation

$$
\begin{aligned}
\textbf{i=1:} & P_1^{n+1} = P_1^n \\
\textbf{i=2:} & P_2^{n+1}\Big(\overline{A} + \frac{\Delta t}{\overline{\overline{R_c}}\Delta x^2}B_{5/2}^n + \frac{2\Delta t}{\overline{\overline{R_c}}\Delta x^2}B_{3/2}^n + \frac{\Delta t}{\Delta x^2}D_{5/2}^n \\
& \quad + \frac{2\Delta t}{\Delta x^2}D_{3/2}^n + \frac{\Delta t}{2\Delta x\overline{\overline{R_c}}}\left(C2_2 + C3_2P_2^n\right)\Big) \\
& \quad + P_3^{n+1}\left(-\frac{\Delta t}{\Delta x^2}B_{5/2}^n - \frac{\Delta t}{\Delta x^2}D_{5/2}^n + \frac{\Delta t}{2\Delta x\overline{\overline{R_c}}}\left(C2_3 + C3_3P_3^n\right)\right) \\
& \quad = \overline{A}P_2^n + \frac{1}{2}\overline{A}\left(P_3 - P_2\right) - \frac{\Delta t}{2\Delta x\overline{\overline{R_c}}}\left(C1_2 + C1_3\right) + \frac{\Delta t}{\Delta x\overline{\overline{R_c}}}C1_1 - \frac{3\Delta t}{2\Delta x}\left(E_3 - E_1\right) \\
& \quad + P_1^n\left(\frac{2\Delta t}{\overline{\overline{R_c}}\Delta x^2}B_{3/2}^n + \frac{2\Delta t}{\Delta x^2}D_{3/2}^n + \frac{\Delta t}{\Delta x\overline{\overline{R_c}}}\left(C2_1 + C3_1P_1^n\right)\right) \\
\textbf{i=N-1:} & P_{N-1}^{n+1}\Big(\overline{A} + \frac{2\Delta t}{\overline{\overline{R_c}}\Delta x^2}B_{N-1/2}^n + \frac{\Delta t}{\overline{\overline{R_c}}\Delta x^2}B_{N-3/2}^n + \frac{2\Delta t}{\Delta x^2}D_{N-1/2}^n \\
& \quad + \frac{\Delta t}{\Delta x^2}D_{N-3/2}^n - \frac{\Delta t}{2\Delta x\overline{\overline{R_c}}}\left(C2_{N-1} + C3_{N-1}P_{N-1}^n\right)\Big) \\
& \quad + P_{N-2}^{n+1}\left(-\frac{\Delta t}{\overline{\overline{R_c}}\Delta x}B_{N-3/2}^n - \frac{\Delta t}{\Delta x}D_{N-3/2}^n - \frac{\Delta t}{2\Delta x\overline{\overline{R_c}}}\left(C2_{N-2} + C3_{N-2}P_{N-2}^n\right)\right) \\
& \quad = AP_{N-1}^n - \frac{1}{2}\overline{A}\left(P_{N-1} - P_{N-2}\right) + \frac{\Delta t}{2\Delta x\overline{\overline{R_c}}}\left(C1_{N-2} + C1_{N-1}\right) \\
& \quad - \frac{\Delta t}{\Delta x\overline{\overline{R_c}}}C1_N - \frac{3\Delta t}{2\Delta x}\left(E_N - E_{N-2}\right) \\
& \quad + P_N^n\left(\frac{2\Delta t}{\overline{\overline{R_c}}\Delta x^2}B_{N-1/2}^n + \frac{2\Delta t}{\Delta x^2}D_{N-1/2}^n - \frac{\Delta t}{\Delta x\overline{\overline{R_c}}}\left(C2_N + C3_NP_N^n\right)\right) \\
\textbf{i=N:} & P_N^{n+1} = P_N^n.
\end{aligned}
$$

4.2.4 Explicit saturation equation

Now that we have calculated the pressure, we can use this to update our masses using the upscaled mass conservation equations

$$
\begin{aligned}
\Phi\frac{\partial M_c}{\partial t} + \frac{\partial}{\partial x}F_{M_c} &= 0 \\
\Phi\frac{\partial M_w}{\partial t} + \frac{\partial}{\partial x}F_{M_w} &= 0.
\end{aligned}
$$

These are transport equations, and can be discretised like

$$
\frac{{M_{c_i}}^{n+1} - {M_{c_i}}^n}{\Delta t} + \frac{{F_{M_c}}_{i+1/2}^{\ n} - {F_{M_c}}_{i-1/2}^{\ n}}{\Phi\Delta x} = 0 \tag{4.14}
$$

$$\frac{{M_w}_i^{n+1} - {M_w}_i^n}{\Delta t} + \frac{{F_{M_w}}_{i+1/2}^n - {F_{M_w}}_{i-1/2}^n}{\Phi \Delta x} = 0 \tag{4.15}$$

We now need to calculate the saturation in each cell or equivalently, the height of the interface between CO_2 and brine, h. We have the two definitions of the mass per volume

$$M_c = R_c S_c = R_c \frac{H-h}{H}(1 - s_{wr}) \tag{4.16}$$

$$M_w = \rho_b S_b = \rho_w \left(\frac{h}{H} + \frac{H-h}{H} s_{wr} \right), \tag{4.17}$$

and we can use any of these to calculate the saturation. To begin with, we use (4.17). Rewriting this equation we get

$$h = \frac{M_b H - \rho_w H s_{wr}}{\rho_w - \rho_w s_{wr}}. \tag{4.18}$$

4.2.5 Volume correction

In an ideal case, we would get the same value for the height of the interface whether we calculate it using the mass of brine or the mass of CO_2. However, once we start making approximations by discretising the differential equations, the world stops being perfect. Therefore, we observe a slight deviation in the two calculated values. We therefore include a correction term when we solve our pressure equation to account for this difference. We denote h_1 as the value for the interface we get when we calculate it using the mass of brine, and h_2 the value we get when we use the mass of CO_2. Then we define the volume correction $\Delta V = h_1 - h_2$. We can then include the volume correction term in the pressure equation

$$A\frac{\partial P}{\partial t} - \frac{1}{R_c}\frac{\partial}{\partial x}\left[B\frac{\partial P}{\partial x} - C \right] - \frac{\partial}{\partial x}\left[D\frac{\partial P}{\partial x} - E \right] = \frac{-\Delta V}{H\tau\Delta t} \tag{4.19}$$

where the term τ says how fast we want this volume error to disappear. Setting $\tau = 1$ may seam like an ideal choice, but has proven to give some problems with the stability, so we choose to set $\tau = 2\pi$.

4.3 Stability

The stability of the method used to discretise our pressure equation depends on the stability of each term in the discretisation. We have used an implicit control volume method which is stable for all time steps, and a partially

implicit Lax-Friedrichs' method. The limiting case term in our discretisation is therefore the Lax-Friedrichs' part. We will now look at the stability of the explicit Lax-Friedrichs' method. It can be shown similarly that the same stability demand applies for the implicit method, so we expect our partially implicit method to have this same stability demand.

4.3.1 Lax-Friedrichs' method

Conditions for convergence

Theorem 1 gives us some conditions which a method must fulfil in order to converge to the correct solution of the partial differential equation [*Aavatsmark*, 2004]

Theorem 1. *The solution of a flux consistent conservation method which is monotone converges to the unique entropy solution of the differential equation.*

Local convergence

Since the method is supposed to solve a conservation law, it needs to express local conservation. This means that what flows out of one cell needs to flow into the neighbouring cell, which we can express as

$$\frac{u_i^{n+1} - u_i^n}{\Delta t^{n+1}} + \frac{\phi(u_i^n, u_{i+1}^n) - \phi(u_{i-1}^n, u_i^n)}{\Delta x_i} = 0 \tag{4.20}$$

for explicit methods. We see directly from (4.11) that the explicit Lax-Friedrichs' method is on local conservation form.

Flux consistency

To get flux consistency, the discrete flux ($\phi(u_L, u_R)$) has to approximate the flux of the differential equation ($f(u)$) such that

- $\phi(u, u) = f(u)$
- $|\phi(v_1, v_2) - f(u)| \leq k \max\{|v_i - u|\} \forall v_i s.t. |v_i - u| < \epsilon$

Monotonicity

An explicit method can be written as the system $\mathbf{u}^{n+1} = \mathbf{G}(\mathbf{u}^n)$.

Theorem 2. *An explicit method is monotone if the Jacobian matrix*

$$\mathbf{G}'(\mathbf{u}) \geq 0.$$

Lax-Friedrichs' method can be written as $\mathbf{u}^{n+1} = \mathbf{G}(\mathbf{u}^n)$ if we define

$$G_i(u) = \frac{1}{2}(u_{i-1} + u_{i+1}) - \frac{1}{2}\frac{\Delta t}{\Delta x}\left[f(u_{i+1}) - f(u_{i-1})\right]. \tag{4.21}$$

For this method to be monotone, all $\frac{\partial G_i}{\partial u_j}$ have to be zero or positive. Calculating these values we get

$$\frac{\partial G_i}{\partial u_i} = 0 \tag{4.22}$$

$$\frac{\partial G_i}{\partial u_{i+1}} = \frac{1}{2}\left(1 - \frac{\Delta t}{\Delta x} f'(u_{i+1})\right) \tag{4.23}$$

$$\frac{\partial G_i}{\partial u_{i-1}} = \frac{1}{2}\left(1 + \frac{\Delta t}{\Delta x} f'(u_{i+1})\right). \tag{4.24}$$

Equations (4.22) and (4.24) are always zero or positive, but for (4.23) to be positive, we need to have

$$\frac{\Delta t}{\Delta x}\|f'\|_{L^\infty} \leq 1 \tag{4.25}$$

which we recognize as the CFL-condition. The explicit Lax-Friedrichs' method is therefore monotone under the CFL-condition, and will then by Theorem 1 converge to the solution of the differential equation.

Chapter 5

Results

5.1 Model problem

As described in the first chapter, we inject CO_2 in aquifers that are deep enough to exceed the critical point of CO_2, which is at approximately 31°C and 7.4MPa. For a typical geothermal gradient of 30°C/km, this means that we inject into aquifers at depths greater than 800m. The supercritical CO_2 is significantly denser than gaseous CO_2, and has both gas- and fluid-like properties [*Celia and Nordbotten*, 2012]. Our aquifer is 50 meters thick, 20 km wide, and is tilted with an angle of 0.1°. Other parameters are from *Celia and Nordbotten* [2012] and are shown in Table 5.1. For the relative permeability, I use the Brooks-Corey model where

$$\begin{aligned} k_{rw} &= s_{w,N}^4 \\ k_{rc} &= 0.4\left(1 - s_{w,N}^2\right)\left(1 - s_{w,N}\right)^2 \end{aligned} \tag{5.1}$$

Properties of the aquifer			
Parameter	*Size*	*Unit*	*Description*
K	10^{-13}	m^2	Permeability
ϕ	0.15		Porosity
Properties of the fluids			
ρ_b	1099	kg/m^3	Density of brine, constant
ρ_0	733	kg/m^3	Density of CO_2 at height H
μ_b	$0.5e-3$	$Pa \cdot s$	Viscosity of brine
μ_c	$0.06e-3$	$Pa \cdot s$	Viscosity of CO_2
s_{wr}	0.2		Residual saturation brine

Table 5.1: Parameters for our model problem

where $s_{w,N} = \frac{s_w - s_{wr}}{1 - s_{wr}}$ is the normalized water saturation [*Brooks and Corey*, 1964].

5.2 Results

Unfortunately, we have not succeeded in solving this problem. We have tried coding up the discretisation described in the previous chapter, but have not been able to get reliable results. We have tried the code on two different test cases, one with an aquifer initially filled with brine (1), and one initially filled with CO_2 (2). In both cases, we expect that nothing will happen, i.e. the solution is stationary.

5.2.1 Test case 1: Initially brine filled aquifer

In this test case, we start out with an aquifer filled completely with brine. There is no CO_2 present in the system, and we therefore have an incompressible system. The result of this simulation is stationary, as we would expect, and is shown in Figure 5.1.

5.2.2 Test case 2: Initially CO_2 filled aquifer

In this test case, we start out with an aquifer filled completely with CO_2. There is only residual brine present in the system. At first, we run the code with no compressibility, and get the results shown in Figure 5.2. As we can see, the solution is stationary, and there does not seem to be any problems here. The results look very much like those in Section 5.2.1, as we would expect, since CO_2 would behave very much like brine when we exclude the compressibility.

We then try to include the compressibility. The result of this simulation with compressibility values of $\beta = 10^{-8}\text{Pa}^{-}1$ is shown in Figure 5.3. As we can see from the figure, there seem to be some problems with the boundary values. We have tried to solve this problem, but have been unsuccessful at this.

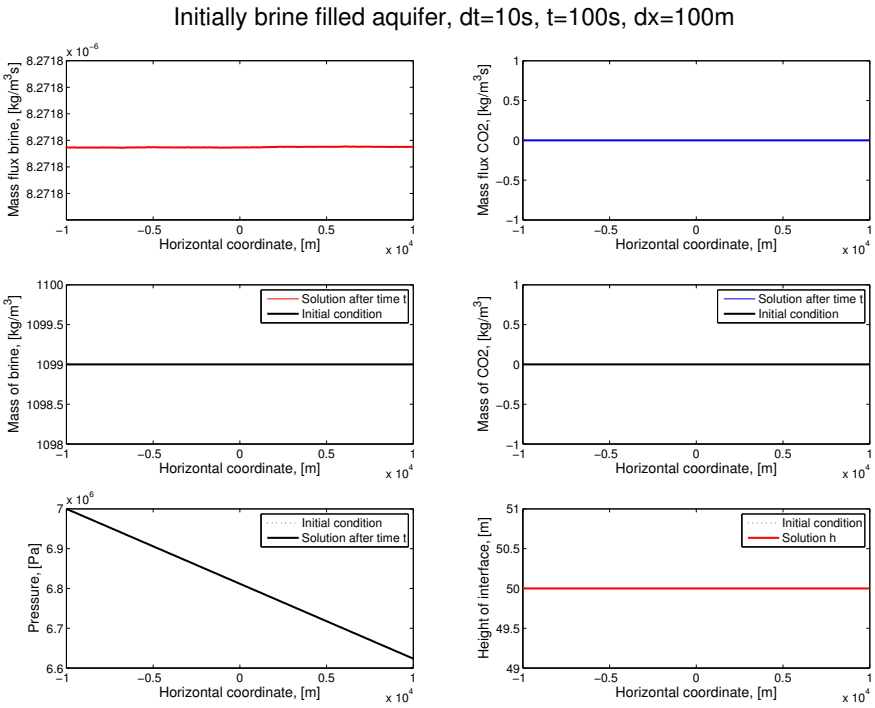

Figure 5.1: Test case 1: Brine filled aquifer.

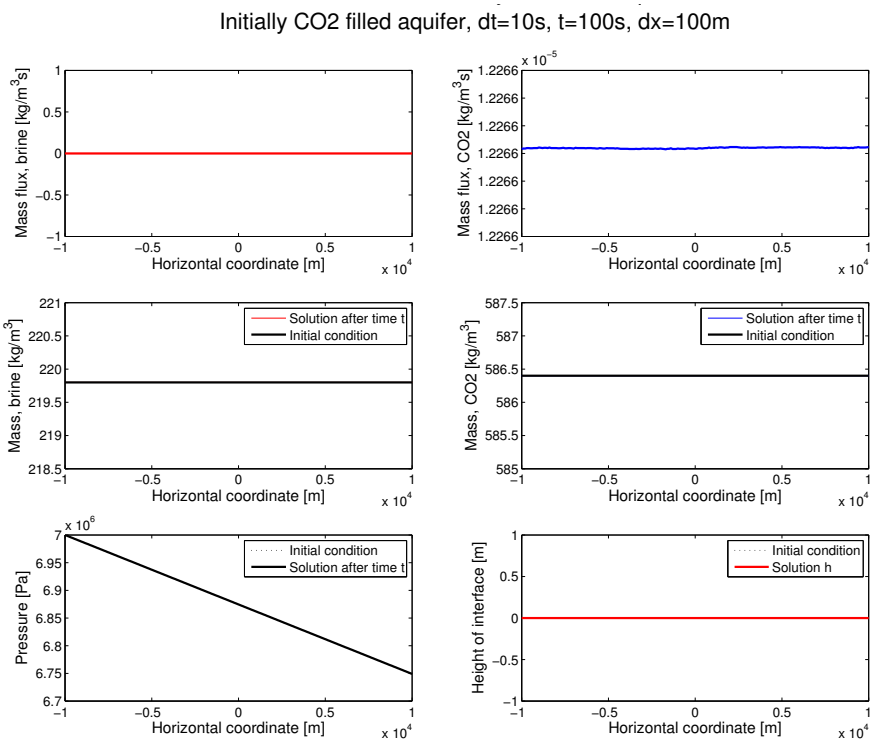

Figure 5.2: Test case 2: CO_2 filled aquifer, without compressibility

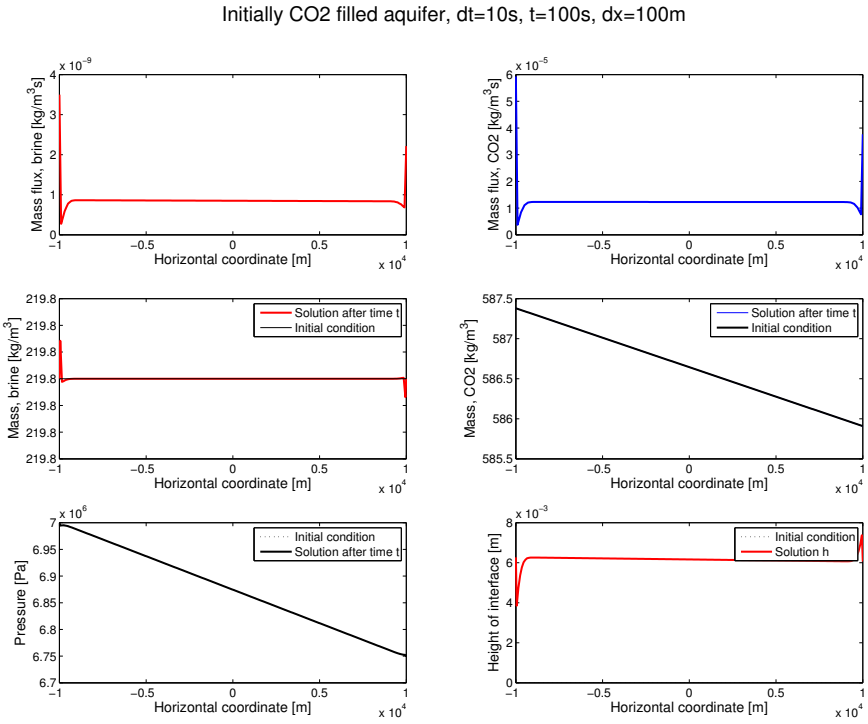

Figure 5.3: Test case 2: CO_2 filled aquifer, with compressibility

Chapter 6

Discussion and Further work

6.1 Discussion

In this thesis, we have derived equations describing CO_2 storage in deep saline aquifers, including compressibility in the CO_2 phase, using a multiscale model where we have vertically integrated the equations to get rid of the vertical dimension. The equations we have derived can be compared to other work on this topic

1. Incompressible flow: Setting $\beta = 0$, we remove all compressibility in the system, and we get back the equations found in other work on incompressible fluids, like *Nordbotten and Dahle* [2011]

2. Quasi compressibility: Some work like *Gasda et al.* [2009] have considered horizontal compressibility in their models. This corresponds to removing the compressibility from the transport terms B and C in Equation (3.27), but keeping it in the accumulation term A.

3. Full model with compressibility: The path chosen in this thesis. Compressibility in included in both the horizontal and vertical direction.

Using this full model with compressibility, our equations become a lot more complicated than they are when using incompressible models, and we have not succeeded in solving this problem. Our full compressible models have been discretised, but we have not been able to implement them correctly. It seems from the results in Chapter 5 like the problem is in the implementation of the boundary conditions, but we have not been able to locate and solve this problem in the time frame available for this thesis.

6.2 Further work

The problem presented in this thesis is definitely an interesting problem, which we hope someone will complete some day. We have identified some points that should be looked at in further work.

First of all we would need to have a working code. To obtain this, we would need to locate and solve the problems with the boundary values. This could either be an error in the discretisation, in the implementation or it could simply be that the numerical methods we have used does do not work on this system.

When we have a code that we think works, we would try to verify this code by comparing it to other works. We could try setting the compressibility to zero, and test it against previous work on incompressible flow, for instance those of *Celia and Nordbotten* [2012] or *Gasda et al.* [2008], or we could remove the vertical compressibility from our model and compare it to works like *Gasda et al.* [2009].

When convinced that our code works, we would like to run it for different test cases, varying parameters like densities, viscosities, permeabilities and so on. We would also like to try realistic parameters for different reservoirs, in particular variations in debts.

At last, we would like to expand the code to a 2D model, and use on more "realistic" geological reservoirs, including fractures, varying thickness, capillary fringe and so on.

It is difficult to say something about what we would expect from these simulations, and which conclusion we could draw from it. We do not think that the the compressibility will always have a huge impact on the result. However, we believe that in some cases, for some reservoirs, it could make a significant difference, which is why we wanted to look at the compressibility in the first place.

Nomenclature

α	Index of fluid phase, $\alpha = c$ or w
β	Compressibility of CO_2
Λ_α	Coarse scale mobility of phase α
λ_α	Fine scale mobility of phase α
$\mathbf{K}$	Permeability of the porous media
μ_α	Viscosity of phase α
ϕ	Fine scale porosity
ρ_α	Fine scale density of phase α
$\hat{R}_c^2$	Coarse scale square density of CO_2
ρ_0	Fine scale scale density of CO_2 measured at a reference point
F_{m_α}	Coarse scale mass flux of phase α
g	Acceleration of gravity
H	Height of the aquifer
h	Height of the interphase between the two fluid phases
$k_{r\alpha}$	Fine scale relative permeability of phase α
P	Coarse scale pressure measured at the interphase
p_0	Fine scale pressure of CO_2 measured at a reference point
R_c	Coarse scale density of CO_2
S_α	Coarse scale saturation of phase α

s_α	Fine scale saturation of phase α
s_{cr}	Residual CO_2 saturation
s_{wr}	Residual brine saturation
u_α	Fine scale Darcy velocity of phase α

Bibliography

Aavatsmark, I., Bevarelsesmetoder for hyperbolske differensialligninger, *University of Bergen*, 2004.

Bachu, S., Sequestration of CO_2 in geological media in response to climate change: road map for site selection using the transform of the geological space into the CO_2 phase space, *Energy Conversion and Management*, *43*, 87–102, 2002.

Britannica, Atmosphere: carbon dioxide concentration, Website, 2012, `http://www.britannica.com/EBchecked/media/69345/Carbon-dioxide-concentrations-in-Earths-atmosphere-plotted-over-the-past`.

Brooks, R., and A. Corey, Hydraulic properties of porous media, *Hydrology Papers, Colorado State University*, 1964.

Celia, M., and J. Nordbotten, *Geological Storage of CO_2: Modeling Approaches for Large-Scale Simulation*, Wiley, 2012.

Chen, Z., G. Huan, and B. Li, An improved impes method for two-phase flow in porous media, *Transport in porous media*, *54*, 361–376, 2004.

Gasda, S., M. Celia, and J. Nordbotten, Upslope plume migration and implications for geological CO_2 sequestration in deep, saline aquifers, *The IES Journal Part A: Civil & Structural Engineering*, *1*, 2–16, 2008.

Gasda, S., J. Nordbotten, and M. Celia, Vertical equilibrium with sub-scale analytical methods for geological CO_2 sequestration, *Computational Geosciences*, *13*, 469–481, 2009.

Lake, L. W., *Enhanced oil recovery*, Prentice-Hall, Inc, 1989.

LeVeque, R., *Numerical methods for conservation laws*, Birkhäuser, 1992.

Nordbotten, J., and H. Dahle, Impact of the capillary fringe in vertically integrated models for CO_2 storage, *Water Resources Research*, *47*, W02,537, 2011.

Nordbotten, J., M. Celia, and S. Bachu, Injection and storage of CO_2 in deep saline aquifers: Analytical solution for CO_2 plume evolution during injection, *Transport in Porous Media*, *58*, 339–360, 2005.

Pettersen, Ø., *Grunnkurs i reservoarmekanikk*, Matematisk institutt-UiB, 1990.

Tans, P., and R. Keeling, Atmospheric CO_2 at mauna loa observatory, Website, 2012, `www.esrl.noaa.gov/gmd/ccgg/trends/`.

Torp, T., and J. Gale, Demonstrating storage of CO_2 in geological reservoirs: the sleipner and sacs projects, in *Kyoto Energy Conference October*, 2002.